



Inhibitory effect of antisense aminopeptidase N (APN/CD13) cDNA transfection on the invasive potential of osteosarcoma cells

Akira Kido, Sabine Krueger, Carsten Haeckel & Albert Roessner
Department of Pathology, Otto-von-Guericke University, Magdeburg, Germany

Received 11 October 2002; accepted in revised form 25 February 2003

Key words: aminopeptidase N (APN/CD13), antisense strategy, metastasis, osteosarcoma

Abstract

Aminopeptidase N (APN/CD13), a Zn^{2+} -dependent ectopeptidase, is localized on the cell surface and functions as a transmembrane protein. Increased expression and activity of APN have been postulated to correlate with the aggressive behavior of several tumor types. In this study, the osteosarcoma cell line MNNG/HOS was stably transfected with an expression vector capable of expressing the antisense transcript of APN. Four stably transfected clones, the control clones and parental cells were characterized. Stable integration of the antisense vector was confirmed by PCR analysis of genomic DNA. Competitive RT-PCR revealed that mRNA expression of antisense-transfectants was decreased to approximately 37% of the control cell line. The activity assay showed that the enzymatic activity of APN was inhibited to approximately 51% of the control cell line. Antisense-transfection had no influence on the cellular proliferation measured by the 3-(4,5-dimethylthiazol-2-yl)-2,5-diphenyltetrazolium bromide (MTT) assay, on the motility in Transwell chambers, and on the adhesive potential to collagen I. However, an *in vitro* invasion assay revealed a significant decrease in the number of cells that migrated through a reconstituted membrane (51% of the control cell line). The adhesive potential to Matrigel was also affected (73% of the control cell line). Furthermore, under *in vivo* conditions, a reduced potency to metastasize to the lung was shown in an experimental metastasis assay in nude mice. These findings demonstrate that APN plays an active role in the cellular attachment and proteolytic degradation of the extracellular matrix in the metastatic process of osteosarcomas.

Abbreviation: GAPDH – glyceraldehyde-3-phosphate dehydrogenase

Introduction

During the metastatic process, a tumor cell proliferates, detaches from the primary site, invades the host stroma, enters the circulation, survives and arrests in a distant organ's capillary bed, extravasates into the parenchyme of that organ, and proliferates again [1]. Proteolytic degradation of the extracellular matrix is an important part of this process. Several classes of proteases are implicated, including matrix metalloproteinases [2], serine proteinases [3], cysteine proteinases [4], and aminopeptidases [5].

Aminopeptidase N (APN, CD13), a Zn^{2+} -dependent ectopeptidase localized on the cell surface, is a transmembrane protein that cleaves N-terminal, neutral amino acids of various peptides and proteins [6]. Sequence comparisons of the cloned cDNA revealed that APN is identical to the CD13 antigen, which is the human cluster antigen expressed on the surface of myeloid progenitors, monocytes, granulocytes, and myeloid leukemia cells [7]. APN has been postulated to play diverse tissue-specific roles both in the catalytic and in

the non-catalytic pathway. In synaptic membranes, APN degrades enkephalin and endorphins [8], in the intestinal brush border, this enzyme plays a role in terminating the degradation of peptides as well as in scavenging of amino acids [9]. On vascular cells, APN metabolizes certain vasoactive peptides [10]. In addition, APN has been suggested to play a role in antigen processing and presentation [11]. Cell cycle control and cell differentiation of macrophage/monocyte [12], and mitogenic activation of lymphocytes [13] have been found to be associated with surface APN activity. Furthermore, APN serves as a virus receptor for the corona virus [14], and has recently been reported to be involved in signal transduction with p42/ERK2 MAP kinase in a human T cell line [15].

In malignant neoplasms, APN is considered to influence the mechanism of tumor invasion [16–19]. A variety of cell lines were treated with peptide inhibitors or anticatalytic antibodies, and *in vitro* invasion was investigated [16–19]. Decreased APN activity resulted in a reduced invasion of treated cells in most tumor cell types. However, possible non-catalytic properties of APN, being a key enzyme in the proteolytic cascade of neoplasms, were not found to be affected as reported so far.

Correspondence to: A. Kido, MD, PhD, Department of Orthopedic Surgery, Nara Medical University, 840 Shijo-cho, Kashihara, Nara 634-8522, Japan. Tel: +81-744-223051; Fax: +81-744-256449; E-mail: akirakid@naramed-u.ac.jp

In a wide variety of mesenchymal tumors, APN expression has been already investigated, including osteosarcomas and their relative diseases [20]. With the proteolytic activity, APN may contribute to the high-malignancy of conventional osteosarcomas in the invasion process.

In the present study, we report the direct blocking of APN expression by antisense RNA using the human osteosarcoma cell line MNNG/HOS to provide a more conclusive approach. Stably transfected clonal cell lines were characterized and compared with the parental cell line MNNG/HOS or the control cell line MNNG/TOPO. Invasion, motility and adhesion, as separate steps of metastasis, were evaluated in different functional *in vitro* assays. In addition, cellular malignancy under *in vivo* conditions was investigated in an experimental metastasis assay in nude mice.

Materials and methods

Cell culture

The human osteosarcoma cell line MNNG/HOS was obtained from ATCC (Rockville, Maryland) and tested under mycoplasma-free conditions. The cells were grown under standard conditions in RPMI-1640 (GIBCO, Eggenstein, Germany) and supplemented with 10% heat-inactivated FBS (GIBCO), and antibiotics/antimycotics (GIBCO). They were incubated at 37 °C in a CO₂ incubator, transferred using trypsin/EDTA (GIBCO) and counted using the Coulter counter ZII (Coulter Immunotech, Marseille, France).

Stable transfection of antisense APN gene in osteosarcoma cell line MNNG/HOS

We constructed a transcript that corresponded to a 5'-1015 bp fragment of full-length APN gene (accession no. M22324, nucleotide positions 120 to 1134). The genes for this part of APN were amplified and cloned in antisense orientation into the pcDNA3.1/V5/His-TOPO expression vector according to the manufacturer's instructions (Invitrogen, Groningen, The Netherlands). Sequence analysis showed 100% homology with published sequences for human APN as an antisense orientation. In preliminary experiments, cDNAs containing a 3'-986 bp fragment (nucleotide positions 2061 to 3046) and a middle-973 bp fragment (nucleotide positions 1106 to 2078) were also cloned into pcDNA3.1/V5/His-TOPO. However, in our study, we found the strongest reduction of APN activity using the 5' construct as described above. The empty vector was used as a control plasmid. Transcription was driven by the constitutive cytomegalovirus (CMV) promoter. MNNG/HOS cells (5×10^5) were transfected with 1 μ g of expression vectors using Lipofectin (GIBCO, Eggenstein, Germany) according to the manufacturer's instructions. Cultures were grown in RPMI-1640/FBS for 48 h. Geneticin (GIBCO) was then added to a final concentration of 500 μ g/ml. Selection medium was changed every four days for five weeks. Fifteen resistant cell clones for each antisense transfectant were randomly chosen, isolated and characterized.

Construction of the internal standard RNA of APN

The internal competitive standard RNA was obtained using the method designed by Kehlen et al. [21] In brief, composite primers were synthesized (Primer 1: 5'-GTG ATG GCA GTG GAT GCA CTA GCT TCC TGT CCG AGG ACG TA-3', primer 2: 5'-GAT TTA GGT GAC ACT ATA GAA TAC GTG ATG GCA GTG GAT GCA CT-3', primer 3: 5'-GTG ATG GCA GTG GAT GCA CT-3', and primer 4: 5'-CGT CAC ATT GAG GTG CAG CAG-3'). Primer 1 was composed of two specific primers complementary to the coding strand of aminopeptidase N. Primer 2 contained two sequences: one for the SP6 RNA polymerase and another for the specific sequences of primer 1. The purified product of the first polymerase chain reaction (PCR) amplification with primers 1 and 3 was used as a template for the second amplification with primers 2 and 3. The amplified DNA was gel-purified (Genomed, Bad Oeynhausen, Germany) following *in vivo* transcription driven by the SP6 promoter using the transcription system of Boehringer (Boehringer, Mannheim, Germany). The recombinant RNA was quantified by absorbance at 260 nm and was used as an internal standard in the cDNA synthesis and in the competitive PCR reaction.

RNA isolation and cDNA synthesis

Total cellular RNA was isolated from cells by lysis in Trizol reagents (GIBCO BRL, Eggenstein, Germany) according to the manufacturer's instructions. The first strand DNA was synthesized at 37 °C for 60 min using 5 μ g total RNA in the presence of dilutions of internal competitive standard RNA (1000 pg, 500 pg, 100 pg, 50 pg, 10 pg, 5 pg) in 12 μ l DEPC water, 4 μ l 5 \times RT buffer, 1 μ l dNTP mix (10 mM each of dATP, dCTP, dGTP, dTTP), 2 μ l 0.1 M DTT, 0.5 μ l (150 ng) random primer and 1 μ l (200 U/ μ l) Superscript II RT(GIBCO).

Competitive PCR analysis

cDNA (2 μ l synthesized above) was diluted in 50 μ l of reaction solution. PCR reaction was done according to the manufacturer's standard protocol (Qiagen, Hilden, Germany) in a thermal cycler (Maxicycler PTC 100, Watertown, Massachusetts) for 35 cycles of 60 s at 94 °C, 60 s at 57 °C and 60 s at 72 °C with primers 3 and 4. Ten microliters of each reaction product was run on a 1.5% agarose gel containing ethidium bromide (0.1% μ g/ml) in TAE buffer. The relative intensities of the bands corresponding to target (573 bp) and internal standard (434 bp) PCR products were visualized in UV light. The relative amounts of target and internal standard products were calculated after densitometric analysis using Image Master 1D Prime software (Amersham Pharmacia Biotech, Freiburg, Germany). The ratio of standard to target amplification products was graphed as a function of the initial amount of internal standard, and lines were drawn from a linear regression analysis using InStat graph-PAD software (San Diego, California). The initial amount of target was calculated from the point where the amount

of amplified target equals the amount of amplified standard (ratio = 1). Analysis was performed in triplicate.

Enzyme activity

Enzyme activity was assayed using 1.5 mM alanine p-nitroanilide (Ala-pNA) as a substrate for APN. Assays were performed with intact confluent cell monolayers, grown in 48 well plates. Cells were rinsed three times and incubated at 37 °C with pre-warmed substrate for 20 min. The amount of p-nitroaniline formed was measured in the supernatant by reading at an OD of 405 nm by ELISA reader (Anthos Labtec Instruments, Saltzburg, Austria). Assays were run in triplicate; cell-free and substrate-free blanks were run in parallel. The cells were detached from the tubes and counted. Enzyme activities were expressed as pkat/10⁶ cells.

PCR analysis for genomic DNA

To confirm the stable integration of expression vectors, PCR analysis was performed on genomic DNA from transfectants. High molecular weight DNA was isolated from cells by standard methods. DNA (1 µg) was diluted in 10 µl of the reaction solution. PCR reaction was done according to the manufacturer's standard protocol (Qiagen) in a thermal cycler (Maxicycler PTC 100) for 35 cycles of 60 s at 94 °C, 60 s at 60 °C and 60 s at 72 °C with T7 primer (5'-TAA TAC GAC TCA CTA TAG GG-3'), and a specific primer for 3'-end of inserted antisense fragment (5'-CAT GGC CAA GGG CTT CTA-3'). Ten microliters of each reaction product was run on a 1.5% agarose gel containing 0.1% µg/ml ethidium bromide in TAE buffer. In preliminary experiment, we confirmed the consistency of this method, PCR analysis for the specific sequences of the inserted fragments, with data from Southern blot analysis (data not shown).

3-(4,5-dimethylthiazol-2-yl)-2,5-diphenyltetrazolium bromide (MTT) assay

The succinate dehydrogenase inhibition test (SDI test) using MTT was used. A single cell suspension obtained following treatment with 0.25% trypsin-EDTA was incubated at 37 °C for 3 h, 6 h, 12 h, 24 h or 48 h in a 96-well culture plate. Then 0.1 M sodium succinate and 0.4% 3-(4,5-dimethylthiazol-2-yl)-2,5-diphenyltetrazolium bromide (MTT) (Sigma Chemical Co., St. Louis, Missouri) were added to each well. After further incubation at 37 °C for 2 h, formazan formed from MTT was extracted by adding dimethylsulfoxide and mixing for 15 min. The absorbance was measured at 562 nm using ELISA reader (Anthos Labtec Instruments). All experiments were performed in quadruplicate.

In vitro adhesion assay

Cellular adhesion to matrices of purified collagen I and Matrigel was quantified. Matrices were reconstituted by standard methods in 24 well culture dishes at a concentration of 10 µg/ml collagen I and 10 µg/ml Matrigel. All proteins were diluted in an adhesion buffer (0.25% BSA in

Hank's balanced salt solution), in which tumor cells were resuspended and added to the wells at a concentration of 1 × 10⁵ cells/well. After 45 min at 37 °C in a CO₂ incubator, unattached cells were removed by discarding the medium. Each well was washed twice with adhesion buffer. Adherent fraction was harvested with trypsin/EDTA and the cell number was counted with the Coulter counter (Coulter Immunotech).

In vitro invasion and motility assay

The invasive potential of the tumor cells was evaluated using Transwell chambers (1 cm²/well, Costar, Bodenheim, Germany). The upper and lower culture compartments were separated by polycarbonate filters (12 µm pores). Before the invasion assay, filters were coated with Matrigel (Beckton Dickinson, Heidelberg, Germany), diluted 1:20 in culture medium (final concentration of 250 µg/well). Tumor cells were seeded onto reconstituted basement membrane for 48 h at a concentration of 1 × 10⁵/well. Motility of cells was evaluated in Transwell chambers with uncoated filters of 8 µm pores. Cells were incubated directly onto the filters for 24 h at a concentration of 2 × 10⁴/well. Cells that passed the synthetic basement membranes and polycarbonate filters were harvested by incubating the lower sides of filters with trypsin/EDTA. The numbers of cells were counted using the Coulter counter (Coulter Immunotech).

In vivo experimental metastasis assay

The mice utilized in these experiments were eight-week-old female athymic nudes (Ncr nu/nu). Animal care was provided in accordance with the institutional guidelines for the animal welfare (authorization No. G 0247/98, Germany). Four mice were used per one clone. 2 × 10⁶ tumor cells in a volume of 200 µl each were injected in the tail vein of mice. Animals were killed by dislocation of the cervical vertebra when they appeared distressed or after six weeks. Lungs and livers were subjected to either histological analysis (hematoxylin and eosin) or DNA extraction. After DNA extraction, DNA (250 ng per reaction) was used for PCR analysis in a thermal cycler (Maxicycler PTC 100) with a pair of primers for human β-globin (5'-AGA GCC ATC TAT TGC TTA CA-3', and 5'-TAT GAC ATG AAC TTA ACC AT-3'). The reaction was done in 40 cycles of 60 s at 94 °C, 60 s at 56 °C and 60 s at 72 °C. PCR products were run on 1.2% agarose gel containing ethidium bromide (0.1% µg/ml) in TAE buffer. Semiquantitative analysis was performed using Image Master 1D Prime software (Amersham Pharmacia Biotech) after electronic scanning of the gels. The procedure of DNA extraction was also confirmed by PCR analysis with a pair of glyceraldehyde-3-phosphate dehydrogenase (GAPDH) primers, which can amplify both human and mouse-derived DNA.

Statistics

Statistical analyses were performed using a personal computer and InStat graphPAD software (San Diego, California). To assess the statistical significance of inter-clone

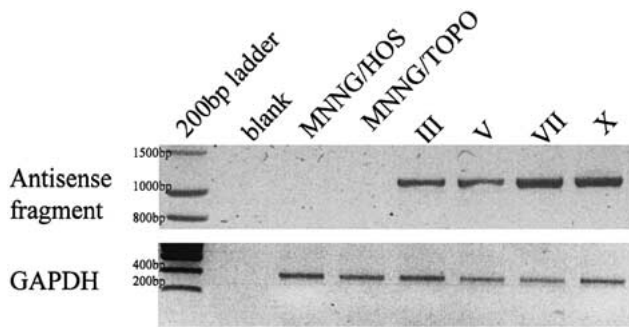


Figure 1. PCR analysis for genomic DNA of MNNG/HOS, MNNG/TOPO and transfectants. Genomic DNA was isolated from all cell clones and amplified with T7 primer and an antisense fragment specific primer. Antisense-specific bands indicating the stable integration of the constructs into the cellular genome were detected in all antisense clones.

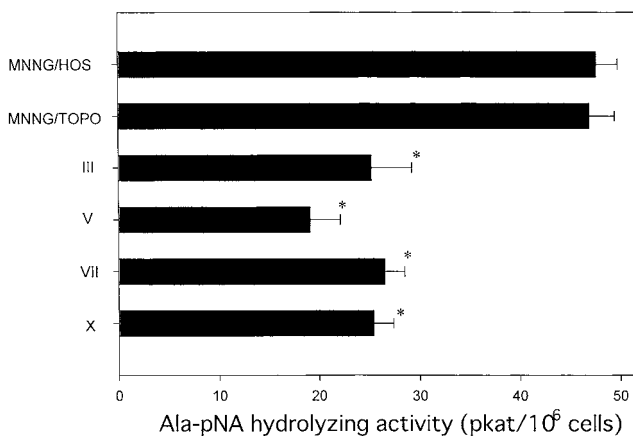


Figure 2. Enzymatic activity was assayed using 1.5 mM Ala-pNA as a substrate for APN. Parental, control or antisense transfected clone cells were incubated with the substrate and the amount of p-nitroaniline formed was measured. *Compared with MNNG/HOS or MNNG/TOPO, APN activity was significantly reduced in all transfectants (two-tailed, unpaired *t*-test; $P < 0.0001$).

differences in quantitative data, Dunnett's multiple comparison test was performed after one-way analysis of variance to determine variations among the group means followed by Bartlett's test to determine the homogeneity of variance.

Results

A 1015 bp fragment of human APN cDNA was subcloned into the expression vector pcDNA3.1/V5/His-TOPO in antisense orientation. For clonal selection, the vector included a geneticin resistance sequence. The construct or negative control (vector without antisense insert) was transfected using lipofection. The transfected cells were grown in the presence of geneticin for 5 weeks. Fifteen resistant clones of antisense transfection were randomly selected for enzymatic activity of APN (results not shown). On screening, the cell clones III, V, VII and X showed the lowest activity of APN. We chose these clonal cell lines for further characterization. As a control, we chose a clone which had a 979 bp of the middle part of APN, in addition to the parental cells with empty vector (MNNG/TOPO). While this clone showed no significant inhibitory effect in any *in vitro* func-

tional analyses, we used it as a non-functional control (clone M).

Characterization of clones III, V, VII and X

Analysis of antisense clones by genomic-PCR demonstrated the stable integration of antisense transcripts into genomic DNA (Figure 1). Compared with the parental cell lines MNNG/HOS and the control transfectant MNNG/TOPO, the antisense clones showed significantly reduced APN activity (Figure 2). Reduction of APN activity was paralleled by a reduced concentration of APN mRNA expression, as demonstrated in competitive RT-PCR analysis (Figure 3). In MTT assay, antisense clones MNNG/HOS and MNNG/TOPO showed similar proliferation activities (Figure 4).

Adhesion on protein matrices

Difference in cellular adhesion between antisense clones and the control cell lines were dependent on the type of protein matrix (Figure 5). Adhesion to collagen I matrices was not influenced by transfection of antisense APN. Out of 1.0×10^5 cells, 63% of MNNG/HOS, 60% of MNNG/TOPO, and 62–67% of antisense clones were adhered to collagen I after 45 min of incubation. In contrast, cellular adhesion of antisense clones to Matrigel was significantly reduced as compared to MNNG/HOS or MNNG/TOPO. On average, 60% of antisense and 82% of MNNG/TOPO clones adhered to Matrigel.

Invasion of antisense APN clones

In vitro invasion assay was designed to investigate whether transfection of antisense APN altered the invasive potential of tumor cells on reconstituted basement membranes in Transwell chambers. To separate the cell clones, we chose stringent assay conditions with a filter pore size of 12 μ m and relatively thick coating with Matrigel (250 μ g/well). Under these conditions, significant cellular invasion was detectable after an incubation period of 48 h. Cellular invasion of antisense clones was significantly lower than the invasive potential of the parental MNNG/HOS line and MNNG/TOPO. Out of 1×10^5 cells in each upper chamber component, we detected an average number of 8% antisense clones on the lower side of filters. In comparison, approximately 16% of cells were detected in MNNG/HOS or MNNG/TOPO (Figure 6).

Motility of antisense APN clones

Cellular motility was measured in Transwell chambers with uncoated filter after 24 h incubation. Out of 2×10^4 cells, 30% of MNNG/HOS, 27% of MNNG/TOPO and 24–32% of antisense cells penetrated the polycarbonate filter (Table 1). There was no significant reduction in cell number. Our results showed that cellular motility is not influenced by transfection of antisense APN.

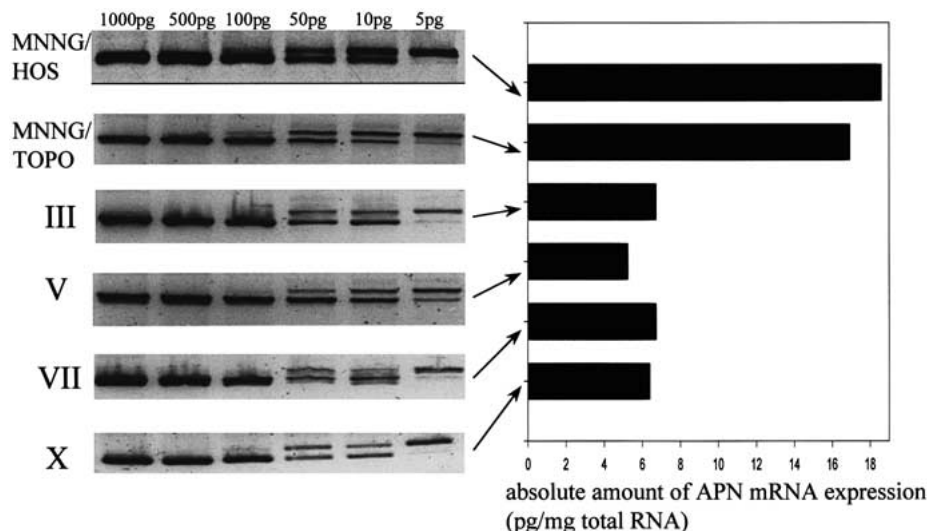


Figure 3. The absolute amounts of mRNA of APN in MNNG/HOS, MNNG/TOPO, and antisense-transfected clones. Competitive RT-PCR was performed in the presence of the internal competitive standard RNA. The initial mRNA amounts were calculated from the point where the amount of amplified target equals the amount of amplified standard after densitometric quantification. In contrast to the parental and control cell lines, APN mRNA expression was significantly reduced in antisense clones III, V, VII and X.

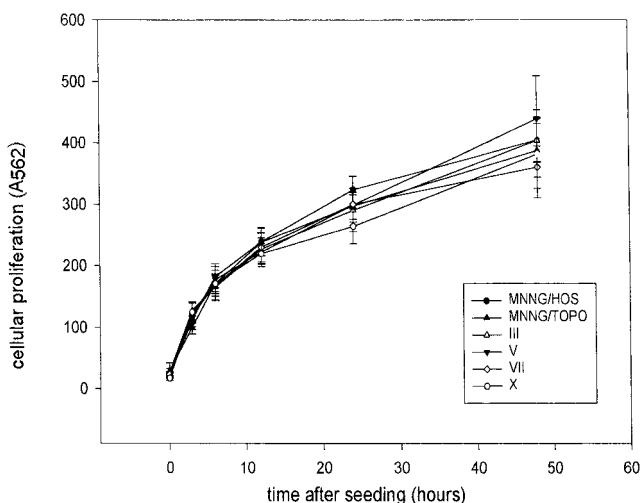


Figure 4. Cellular proliferation of MNNG/HOS, MNNG/TOPO and antisense clones. After incubation, formazan formed from MTT was extracted by adding DMSO and mixing for 15 min; the absorbance was measured. All cell clones showed similar proliferation activities.

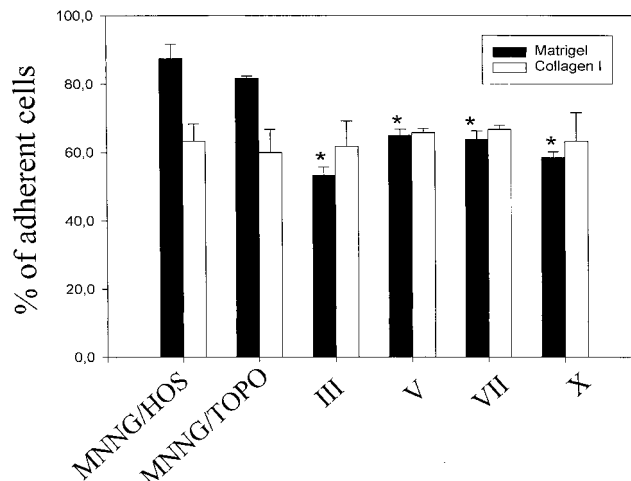


Figure 5. Cellular adhesion of 1×10^5 cells was determined for 45 min on matrices of 10 μ g/ml of Matrigel and collagen I. After stringent washing steps, adherent cells were harvested with trypsin/EDTA and counted using the Coulter counter ZII. *Compared with MNNG/HOS or MNNG/TOPO, cellular adhesion of antisense transfected clones on Matrigel was significantly reduced in all antisense-transfected cells (two-tailed, unpaired *t*-test; $P < 0.005$). Adhesion behavior on collagen I was comparable for all cell lines.

Table 1. Relative cellular motility of MNNG/HOS, MNNG/TOPO, and antisense clones.

Cell Line	% Adherent cells (\pm SD)
MNNG/HOS	29.5 (\pm 3.8)
MNNG/TOPO	27.3 (\pm 2.4)
III	24.7 (\pm 4.2)
V	26.5 (\pm 2.2)
VII	26.6 (\pm 2.4)
X	31.7 (\pm 3.3)

Cells migrating through uncoated filters were harvested by trypsin/EDTA and counted with Coulter counter ZII. Cellular migration was comparable for all cell clones.

Metastasis in nude mice

Because of its most effective inhibitory effect in the *in vitro* functional assays, clone V was used for the nude mice experiment. As controls, MNNG/TOPO and an antisense clone that had a 979 bp of the middle part of APN (clone M) were used. In the *in vitro* functional assays, clone M showed no significant inhibitory effect (data not shown). On routine examinations of organs from the nude mice, significant morphological difference was found only in lungs. The numbers of lung metastatic nodules macroscopically counted are given in Table 2. Besides histological analysis, human β -globin gene was amplified using human-specific primers, from total DNA extracted from the mouse organs

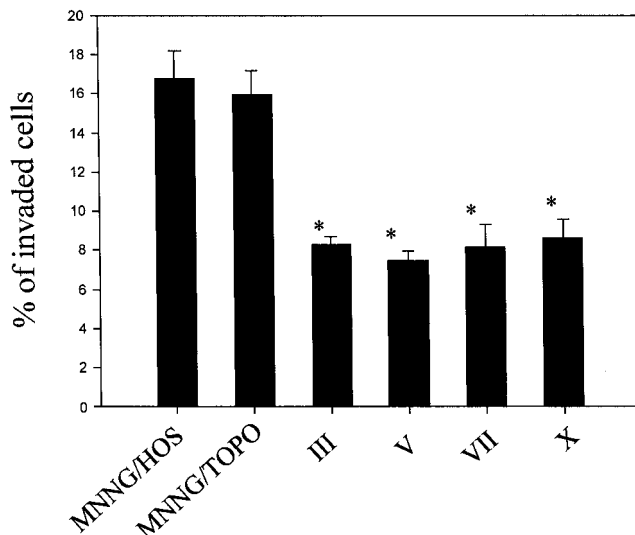


Figure 6. Invasion of MNNG/HOS, MNNG/TOPO and antisense-transfected clones (1×10^5 cells/well) in Matrigel coated Transwell chambers (12 m pores). Cells migrating through reconstituted membrane were harvested by incubation with trypsin/EDTA and counted. *Compared with MNNG/HOS or MNNG/TOPO, invasive potential of all antisense transfectants was statistically reduced (two-tailed, unpaired *t*-test; $P < 0.005$).

Table 2. The number of metastatic nodules in the lung of nude mice.

	No. of metastatic nodules (\pm SD)
MNNG/TOPO ($n = 4$)	120.26 (± 31.04)
M ($n = 4$)	109.16 (± 41.13)
V ($n = 4$)	25.0 (± 10.46) ^a

^aThe value of clone V is significantly smaller than MNNG/TOPO or clone M (two-tailed, unpaired *t*-test; $P < 0.01$).

(Figure 7). In lung samples, the signals of clone V were significantly weaker than those of MNNG/TOPO or clone M (Table 3). We found no human tumor cells in any liver sample (Figure 7).

Discussion

Several groups have previously reported that anticatalytic antibodies or peptide inhibitors for APN markedly inhibited the invasive potential of rodent and human tumor cells [16–19]. Since this protease exerts some influence independent of its enzymatic domain [14, 15, 22, 23], we decided to employ the antisense strategy for APN inhibition. Antisense RNA blocks APN expression at an early stage of mRNA maturation. Thus, this strategy allows us to affect both catalytic and possible non-catalytic functions of APN. In our study, the osteosarcoma cell line MNNG/HOS was stably transfected with constructs that contained a 1015 bp of 5'-fragment in antisense orientation under control of the potent eukaryotic CMV promoter. To exclude possible artifacts of clonal selection, we isolated 15 antisense clones, four of which showed similar growth properties as well as a sufficiently reduced

Table 3. Semiquantitative analysis of the metastasis in lungs of nude mice by PCR amplification of human β -globin in extracted genomic DNA of the mice organ.

	Arbitrary units (\pm SD)
MNNG/TOPO	37.95 (± 3.91)
M	32.04 (± 5.03)
V	6.07 (± 0.65) ^a

Densitometric analysis was performed using Image Master 1D Prime software (Amersham Pharmacia Biotech) after electronic scanning of the gels.

^aThe value of clone V is significantly smaller than MNNG/TOPO or clone M (two-tailed, unpaired *t*-test; $P < 0.0001$).

mRNA expression and enzymatic activity (clone III, V, VII, and X). Since APN is synthesized in a fully active form and unregulated at the cell surface [23], reduced activity may reflect a decreased protein expression of APN.

In general, it cannot be stated with certainty which part of a gene is the best target for antisense strategies. Evaluating three different constructs which corresponded to the 1015 bp of 5'-fragment, 985 bp of 3'-fragment and 979 bp of the middle part of the full-length APN gene in preliminary experiments, we found that the 1015 bp of the 5'-fragment exhibited the strongest and most stable reduction of enzymatic activity of APN. These results, previously observed by others (for review, see [24]), were not totally unexpected; however, the underlying functional mechanisms remain unclear.

The role of APN in cellular proliferation still remains to be clarified. An anti-growth effect was often observed in studies using peptide inhibitors or anticatalytic antibodies for APN in several tumor types [25–27]. Particularly significant effects were noted in leukemic cell lines [26, 27], and one of the inhibitors has even been applied clinically [28]. In contrast to this, Saiki et al. [16] found that although WM15, an anticatalytic antibody, has a potent inhibitory effect on invasion, it did not directly influence tumor cell growth and viability. Two groups have recently reported that peptide inhibitors possess a specific cytotoxicity not mediated by APN [29, 30]. Such an inhibitor-specific toxicity has rarely been reported. Thus, these findings may help to explain the inconsistency of the growth inhibitory effect seen in several inhibitory methods. In our study, direct blocking of mRNA maturation by antisense RNA of APN did not influence the proliferation of osteosarcoma cells for 72 h (Figure 4).

Antisense clones showed a significant reduction of the invasive potential in *in vitro* invasion assays. Lower expression of APN in antisense clones led to a significantly reduced cellular adhesion to Matrigel, but not to collagen I (Figure 5). Cellular motility was not influenced either (Table 1). Therefore, we think that APN contributes to tumor malignancy with proteolytic degradation of and cellular attachment to the Matrigel component. These findings are in line with the study of Fujii et al. [18], who transfected two melanoma cell lines with an expression vector contain-

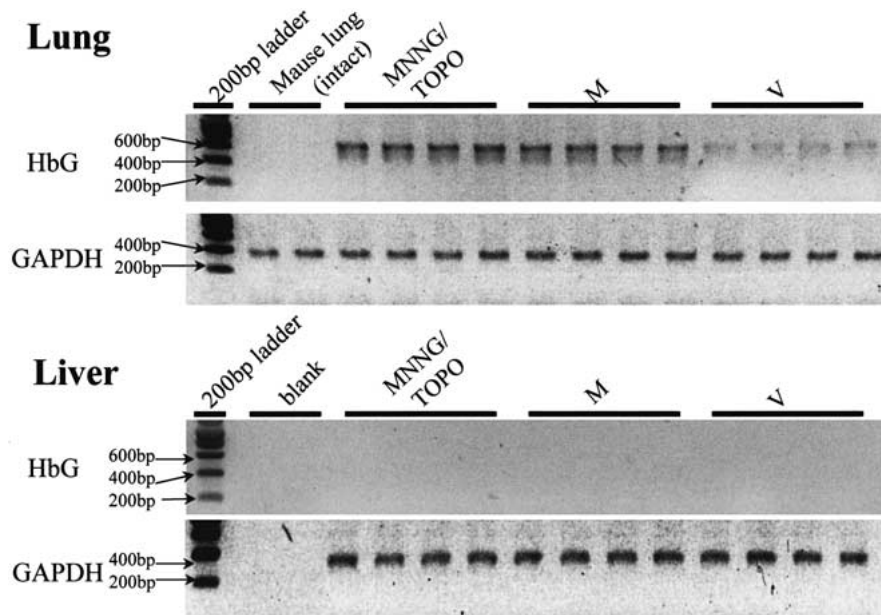


Figure 7. Semiquantitative PCR analysis for human β -globin (HbG). The lanes for intact mouse lung (non-treated mouse) show cross reactivity of the GAPDH primers for mouse genomic DNA, and the specificity of the HbG primers for human genomic DNA. The signals of clone V are significantly weaker than those of MNNG/TOPO or clone M.

ing full length cDNA in sense orientation. Higher expression of APN led to an increase in the invasive potential, type IV collagenase activity, and adhesion to Matrigel, but not in cellular growth. Furthermore, they performed *in vitro* digestion of Matrigel and speculated that the main target of APN was entactin/nidogen, a component of the basement membrane. Interestingly, in their study, bestatin did not inhibit cellular adhesion to Matrigel enhanced by sense cDNA transfection. In support of this, another group reported that anti-immune serum for APN did not affect cellular adhesion of tumors [17]. Taken together, the cellular adhesion might be involved in the non-catalytic function of APN.

Blocking of APN expression also resulted in a decreased metastatic potency to the lung under *in vivo* conditions. Nude mice injected with antisense transfectants showed a reduced amount of human-derived genomic DNA in the lungs (semiquantitative PCR analysis), indicating a lower number of metastatic tumor cells in the organ. In accordance with the results of our experimental metastasis assay, Pasqualini et al. reported that APN is involved in angiogenesis [31], one of the most essential factors causing metastasis. Our antisense strategy might be used for inhibiting angiogenesis to prolong the dormant phase of metastases. However, further investigations are necessary to collect more information on this topic.

In conclusion, APN plays an active role in osteosarcoma cell invasion and metastasis. Reduced expression of APN in the osteosarcoma cell line MNNG/HOS, mediated by antisense RNA, reduced not only the invasive potential but also cellular adhesion. Stable antisense-transfected cell lines provide more precise and specific information of APN functions, which may be one of the possible targets for anti-metastatic strategies in the treatment of osteosarcomas.

Acknowledgements

The authors thank Mr Bernd Wuesthoff for editing the manuscript and Ms Doreen Gaertner for her excellent technical assistance. This work was supported by grants from the Alexander-von-Humboldt Foundation, Germany (to AK, IV-1-7108-JAN) and the Deutsche Forschungsgemeinschaft (SFB 387).

References

1. Nicolson GL. Paracrine and autocrine growth mechanisms in tumor metastasis to specific sites with particular emphasis on brain and lung metastasis. *Cancer Metastasis Rev* 1993; 12: 324–43.
2. Liotta LA, Tryggvason K, Garbisa S et al. Metastatic potential correlates with enzymatic degradation of basement membrane collagen. *Nature* 1980; 284: 67–8.
3. Liotta LA, Goldfarb RH, Brundage R et al. Effect of plasminogen activator (Urokinase), plasmin, and thrombin on glycoprotein and collagenous components of basement membrane. *Cancer Res* 1981; 41: 4629–36.
4. Sloane BF, Honn KV, Sadler JG et al. Cathepsin B activity in B16 melanoma cells: A possible marker for metastatic potential. *Cancer Res* 1982; 42: 980–6.
5. Saiki I, Murata J, Watanabe K et al. Inhibition of tumor cell invasion by ubenimex (bestatin) *in vitro*. *Jpn J Cancer Res* 1989; 80: 873–8.
6. Sanderink GJ, Artur Y, Siest G. Human aminopeptidases: A review of the literature. *J Clin Chem Clin Biochem* 1988; 26: 795–807.
7. Look AT, Ashmun RA, Shapiro LH et al. Human myeloid plasma membrane glycoprotein CD13 (gp150) is identical to aminopeptidase N. *J Clin Invest* 1989; 83: 1299–307.
8. Solhonne B, Gros C, Pollard H et al. Major localization of aminopeptidase M in rat brain. *Neuroscience* 1987; 22: 225–32.
9. Turner AJ, Hooper NM, Kenny AJ. Metabolism of neuropeptides. In Kenny AJ and Turner AJ (eds): *Mammalian Ectoenzymes*. New York: Elsevier Scientific Publishing 1984; 211–42.
10. Ward PE, Benter IF, Dick L et al. Metabolism of vasoactive peptides by plasma and purified renal aminopeptidase M. *Biochem Pharmacol* 1990; 40: 1725–32.

11. Falk K, Rotzschke O, Stevanovic S et al. Pool sequencing of natural HLA-DR, -DQ, and -DP ligands reveals detailed peptide motifs, constraints of processing, and general rules. *Immunogenetics* 1994; 39: 230–42.
12. Koch AE, Burrows JC, Skoutelis A et al. Monoclonal antibodies detect monocyte/macrophage activation and differentiation antigens and identify functionally distinct subpopulations of human rheumatoid synovial tissue macrophages. *Am J Pathol* 1991; 138: 165–3.
13. Amoscato AA, Alexander JW, Babcock GF. Surface aminopeptidase activity of human lymphocytes. I. Biochemical and biologic properties of intact cells. *J Immunol* 1989; 142: 1245–52.
14. Yeager C, Ashmun RA, Williams RK et al. Human aminopeptidase N is a receptor for human coronavirus 229E. *Nature* 1992; 357: 420–2.
15. Lendeckel U, Kahne T, Arndt M et al. Inhibition of alanyl aminopeptidase induces MAP-kinase p43/ERK2 in the human T cell line KARPAS-299. *Biochem Biophys Res Commun* 1998; 9: 5–9.
16. Saiki I, Fujii H, Yoneda J et al. Role of aminopeptidase N (CD13) in tumor-cell invasion and extracellular matrix degradation. *Int J Cancer* 1993; 54: 137–43.
17. Menrad A, Speicher D, Wacker J et al. Biochemical and functional characterization of aminopeptidase N expressed by human melanoma cells. *Cancer Res* 1993; 53: 1450–5.
18. Fujii H, Nakajima M, Saiki I et al. Human melanoma invasion and metastasis enhancement by high expression of aminopeptidase N/CD13. *Clin Exp Metastasis* 1995; 13: 337–44.
19. Kido A, Krueger S, Haeckel C et al. Possible contribution of aminopeptidase N (APN/CD13) to invasive potential enhanced by interleukin-6 and soluble interleukin-6 receptor in human osteosarcoma cell lines. *Clin Exp Metastasis* 1999; 17: 857–63.
20. Mechtersheimer G, Moller P. Expression of aminopeptidase N (CD13) in mesenchymal tumors. *Am J Pathol* 1990; 137: 1215–22.
21. Kehlen A, Gohring B, Langner J et al. Regulation of the expression of aminopeptidase A, aminopeptidase N/CD13 and dipeptidylpeptidase IV/CD26 in renal carcinoma cells and renal tubular epithelial cells by cytokines and cAMP-increasing mediators. *Clin Exp Immunol* 1998; 111: 435–41.
22. Soderberg C, Giugni TD, Zaia JA et al. CD13 (human aminopeptidase N) mediates human cytomegalovirus infection. *J Virol* 1993; 67: 6576–85.
23. Turner AJ. Membrane alanyl aminopeptidase. In Barrett AJ, Rawlings ND and Woessner JF (eds): *Handbook of Proteolytic Enzymes*. San Diego, California: Academic Press 1998; 996–1000.
24. Helene C, Toulme JJ. Specific regulation by antisense, sense and antigene nucleic acids. *Biochim Biophys Acta* 1990; 1049: 99–125.
25. Ino K, Goto S, Okamoto T et al. Expression of aminopeptidase N on human choriocarcinoma cells and cell growth suppression by inhibition of aminopeptidase N activity. *Jpn J Cancer Res* 1994; 85: 923–33.
26. Murata M, Kubota Y, Tanaka T et al. Effect of ubenimex on the proliferation and differentiation of U937 human histiocytic lymphoma cells. *Leukemia* 1994; 8: 2188–93.
27. Lohn M, Mueller C, Thiele K et al. Aminopeptidase N-mediated signal transduction and inhibition of human myeloid cells. *Adv Exp Med Biol* 1997; 421: 85–91.
28. Ota K, Kurita S, Yamada K et al. Immunotherapy with bestatin for acute nonlymphocytic leukemia in adults. *Cancer Immunol Immunother* 1986; 23: 5–10.
29. Sekine K, Fujii H, Abe F. Induction of apoptosis by bestatin (ubenimex) in human leukemic cell lines. *Leukemia* 1999; 13: 729–34.
30. Xu Y, Lai LT, Gabrilove JL et al. Antitumor activity of actinonin *in vitro* and *in vivo*. *Clin Cancer Res* 1998; 4: 171–6.
31. Pasqualini R, Koivunen E, Kain R et al. Aminopeptidase N is a receptor for tumor-homing peptides and a target for inhibiting angiogenesis. *Cancer Res* 2000; 60: 722–7.